PCCP

Accepted Manuscript

ROYAL SOCIETY OF CHEMISTRY

www.rsc.org/pccp

First Principles study of Organic Sensitizers for Dye Sensitized Solar Cells: Effects of Anchoring Groups on optoelectronic properties and Dye aggregation

Santhanamoorthi Nachimuthu, Wei-Chieh Chen, Ermias Girma Leggesse and Jyh-Chiang Jiang*

Department of Chemical Engineering, National Taiwan University of Science and Technology, Taipei 106, Taiwan, R.O.C.

*Corresponding author Tel.: +886-2-27376653. Fax: +886-2-27376644

E-mail address: jcjiang@mail.ntust.edu.tw

Abstract:

We have designed a new set of D-π-A type organic dye sensitizers with different acceptor and anchoring groups and systematically investigated their optoelectronic properties for the efficient dye sensitized solar cell applications. Particularly, we have focused the effects of anchoring groups on the dye aggregation phenomenon. TDDFT results indicate that the dyes with CSSH anchoring groups exhibit improved optoelectronic properties than the other dyes. Further, molecular dynamics simulations have performed to describe the formation of dye aggregation due to intermolecular hydrogen bonding. Observed results indicate that dyes with CSSH anchoring groups are less prone to aggregate because of its very weak intermolecular interactions.

Keywords: Dye Sensitized Solar Cells; Organic Dyes; Density Functional Theory; Absorption Spectra; Molecular Dynamics simulations; Dye Aggregation.

1. Introduction

Over the last two decades, dye sensitized solar cells (DSSCs) have been attracted considerable research attention among the renewable energy sources because of its low cost and high conversion efficiency.[1-3] The dye sensitizer; is most important component in DSSCs, which is not only used to absorb light but also it helps to inject the electrons into semiconductor surface. Recently, metal-free organic dyes have been proposed instead of organometallic dyes due to their high molar extinction coefficients, flexibility of their molecular design, low cost device fabrication and environmental friendliness.[4-7] A typical organic dye consists of an electron donor, π-conjugated spacer, and acceptor with anchoring groups.

Even though a lot of efforts have been made in the designing strategies of organic dyes to enhance the efficiency of DSSCs, one can reach up to only 12 %. These strategies include the substitution of different donor/acceptor moieties and by means of increasing π-spacer or changing anchoring groups. The overall DSSC performances are determined by some key factors such as excited state redox potential of the dyes, electronic coupling between the LUMO and the semiconductor conduction band and more importantly the formation of dye aggregation. Most of the above issues have been solved by means of substituting different functional groups and their performances were reported in the literature except dye aggregation. In organic dyes, aggregation occurs when it adsorbs on the

semiconductor surface, which lowers the conversion efficiency.[8-12]

Electrostatic and non-covalent interactions of the organic dyes with the surface or within the adjacent dye molecules cause the dye aggregation. Previous studies show that aggregation can be controlled either by means of substituting bulky groups or by bridging of two chromophores into spiral configuration.[13-15] Also, some anti-aggregating agent has been used to avoid the formation of aggregation, which leads to improve the electron transport and thereby increase in the power conversion efficiency of DSSCs. [16-18] All of these studies and others which are previously reported in the design of efficient sensitizers for DSSCs used either carboxylic acid or cyanoacrylic acid as an anchoring group, which may increase the dye aggregation.[4, 5, 19] The anchoring group plays an important role not only in the electron injection part but also in governing the dye aggregation. However, the effect of anchoring groups on the dye aggregation have been much less investigated. In recent years, theoretical studies are used to investigate the different atomic structures and certain dynamics processes of dye aggregation, which cannot be easily observed experimentally. Feng et.al[20] reported the aggregation effects on optoelectronic properties of organic dyes. Hitoshi et.al[21] investigated the aggregation of black dyes via intermolecular hydrogen bonding using DFT methods. In the present study, we designed the D-π-A structured organic dyes with new set of anchoring groups such as PO_3H_2, SO_3H and CSSH. Furthermore, the substituent effect of cyano group (CN) with these anchoring groups on the aggregation and absorption properties have been

investigated. Herein we focus the formation of dimers via intermolecular hydrogen bond in the designed dyes using MD simulations.

2. Computational Details:

The geometries of designed dyes with different acceptor and anchoring groups were optimized using both the B3LYP,[22] and ωB97XD[23-26] hybrid exchange correlation functionals together with a standard 6-31G* basis set.[27] Further, frequency calculations have been performed at the same level of theories to verify the nature of the saddle point. The accuracy of different DFT functionals (such as B3LYP, BHandHLYP[28] M062X,[25] CAM-B3LYP[26] and BHandHLYP[28]) for the spectral properties have been explored by performing the benchmark calculations for some of the organic dyes (L1 and L2)[29] which are similar to our designed dyes in the acetonitrile environment and the calculated absorption energies are summarized in Table S1 of supporting information. In order to include the solvent effects in benchmark calculations, conductor-like polarizable continuum model (CPCM) method was used.[30, 31] As can be seen from the Table S1, ωB97XD method gives the absorption energies closer to the experimental values for the referenced dyes. Recent previous studies [32, 33] also confirm that the accuracy of this method in predicting the vertical excitation energies. Hence, we considered the long range corrected ωB97XD method to calculate the lowest 8 singlet transitions for all of our designed dyes. Further, the calculated absorption energies were transformed into spectra in the SWizard program,[34, 35] using Gaussian model with half-

bandwidths of 3000 cm^{-1}. All the above calculations were performed using the Gaussian09 package.[36]

2.1. MD simulation Details:

Molecular dynamics simulations were performed using FORCITE Module which is commercially available in Materials Studio v7 package[37] with the Condensed-Phase Optimized Molecular Potential for Atomistic simulation studies (COMPASS) force field.[38-40] A 37.02 Å and 36.19 Å cubic simulation box with periodic boundary conditions in all directions was constructed with a density of 1g/cm^3 for dyes with COOH and CSSH anchroing groups, respectively. The systems were minimized using smart algorithm with 5000 integration step. To equilibrate the systems, a molecular dynamics simulations were carried out under canonical ensemble (NVT) at a constant temperature of 298 K by using Andersen thermostat. The equations of motion were integrated with the velocity Verlet algorithm for a total simulation time of 2ns with a time step of 1fs. The systems were equlibrated further by performing annealing for 5 cycles using anneal task in FORCITE module. In this process, the temperature was increased from 300K to 500K with 5 heating ramp/cycle. A production run of 500ps was carried out under isothermal–isobaric (NPT) conditions, with pressure and temperature held at 1atm and 300 K, respectively, by employing Nose thermostat and Berendsen barostat. During the simulations, the non-bonded energies were calculated using the popular Ewald summation while the COMPASS force

field was used to calculate both van der Waals and electrostatic interactions.

3. Results and Discussion:

The organic dyes based on D-π-A configuration considered in this study are shown in Figure 1. Here, we considered 4-methoxy-N-(4-methoxyphenyl)-N-phenylbenzeneamine (MPBA) as donor, thiophene (T) as π-bridge, three acceptors, such as dicyanomethylidene-cyclopentadithiophene (CDM), cyclopentadithiophene (CDT), and thienopyrazine (TP), and four anchoring groups such as COOH, CSSH, PO_3H_2, and SO_3H and all of these molecular structures are shown in the Figure 1. From our previous study, the strength of the considered acceptors is as follows; CDM > TP > CDT. [5] Then the basic D-π-A configuration has been constructed using the above moieties and optimized using both B3LYP and ωB97XD with 6-31G* basis set. Also, the effects of cyano group in the anchoring part have been studied.

3.1. Optoelectronic Properties:

The UV/vis spectra of these designed sensitizers were simulated in the gas phase using ωB97XD/6-31G* level of theory based on the ground state optimized structures at same level of theory. The simulated UV/vis spectra of these designed sensitizers are shown in Figure 2 and the corresponding features for the main peak of the spectra of dyes with COOH and CSSH anchoring groups are summarized in Tables 1 and 2, respectively. The spectral data of dyes with other anchoring groups calculated at ωB97XD/6-31G* level of theory are

given in Tables S2 and S3 of Supporting Information.

It has been observed from Figure 2, the simulated spectra of the designed sensitizers with CDM acceptor groups possess dual band absorption peaks; one in shorter wave length region (~345-410 nm) and another one in longer wavelength region (~630-660 nm), whereas, mono band absorption observed in the case of sensitizers with CDT and TP acceptor groups. This result confirms our earlier conclusion that the strength of the acceptor influences the UV/vis spectra.[5] Also, we compared the effect of different anchoring groups on the absorption spectra. From Figure 2a-c, it has been observed that the simulated absorption spectra of the sensitizers with COOH, PO_3H_2, and SO_3H anchoring groups are almost similar, whereas, the sensitizers with CSSH anchoring group (Figure 2d) possess absorption peaks at longer wavelength regions also. Further, to know the effect of substitution of the cyano group in the anchoring part, we calculated the absorption properties of designed dyes with cyano group and the simulated spectra are also included in Figure 2. We found that the inclusion of cyano group makes the absorption spectra red shifted in the shorter wave length regions and slightly increased the intensity of the spectra of all the designed dyes which are in accordance with our previous studies.[5, 19]

3.2.Frontier Molecular Orbitals:

To understand further, we plotted the molecular orbital (MO) diagram which determines the charge separated states of the designed dyes and are shown in Figure 3 for

dyes with COOH and CSSH anchoring groups and for other systems are given in Figures S1-S3 of supporting information. It is well known that, for an efficient dye, the HOMO must be localized on the donor part and LUMO on the acceptor and anchoring groups.[5, 41] From this plot, we observed that the LUMO of the dyes with strongest acceptor (CDM) localized mainly on the acceptor moiety not in the anchoring groups, hence the electron injection efficiency from the anchoring group to the semiconductor surface will be less even though it has absorption band in the visible region. This may be due to the strongest electron accepting ability of CDM, hence it will trap all the excited electrons. Whereas, LUMO of TP and CDT acceptor groups localized both on the acceptor and anchoring groups which will be having more electron injection ability. The calculated molecular orbital compositions of designed dyes with CSSH and COOH anchoring groups are summarized in Table 3, which shows that the HOMOs are mainly contributed by the donor and π-bridge subunits and LUMOs are either from acceptor or anchoring groups. Our previous study reveals that contributions from anchoring groups for LUMOs is significant to inject the electrons into the semiconductor surface.[41] From Figures S2& S3, we can see that the LUMOs of the dyes with PO_3H_2 and SO_3H_2 anchoring groups, delocalized only on the acceptor part and hence, it will not inject the electrons into the semiconductor surface efficiently. Further from table 3, we found that our designed dyes with CSSH anchoring groups contributed to LUMOs significantly larger than the COOH anchoring groups. The contribution of COOH anchoring groups to LUMOs is

only 10% whereas CSSH anchoring group contribution is ~ 50%. Therefore, we expect that dyes with CSSH anchoring groups will have strong electronic coupling with the semiconductor surface, and it can easily inject the excited electrons into the surface than dyes with COOH groups. Based on the above results, we considered only dyes with CSSH and COOH anchoring groups for the further calculations.

Figure 4 shows the calculated energy levels of the designed dyes with different acceptor and anchoring groups (CSSH and COOH). As the strength of the acceptor group decreases, the HOMO-LUMO gap increases. It has been observed that the LUMO level is downshifted with an increase in the strength of the acceptor. Whereas, the HOMO level does not change much since, the HOMO is mainly localized on the donor and π-bridge part. The calculated HOMO-LUMO gap for the dyes with CSSH anchoring group is lower than the COOH group which is responsible for the redshift in UV/vis absorption spectra of the dyes with CSSH anchoring groups. Also, the substitution of cyano group into the anchoring group decreases the HOMO-LUMO gap value further in the designed dyes. Based on the previous studies,[41-43] we expect that the sensitizers having smaller HOMO-LUMO energy gap values will show higher efficiency and hence the designed dyes with CSSH anchoring group may exhibit better performance than the others.

3.3.Dye Aggregation:

Dye aggregation is a well-known concern for DSSC since it leads to a reduced electron injection yield and thereby affects the overall conversion efficiency. [20, 44] Previously many studies reported that the spectral properties of the dyes affected when it forms dimer due to the intermolecular interactions.[45, 46] Generally, dye aggregation is classified into two types; J-type, which causes redshift and H-type aggregation which leads to a blue shift in the UV/vis spectrum. [47, 48] These two kinds (J or H) of aggregation are formed when the dye molecules are stacked side-by-side or face-to-face, respectively. For instance, H type is formed via intermolecular hydrogen bonds between their anchoring groups (usually –COOH groups), when it forms the dimer or trimer. Keeping in this mind, here we investigate the possibility of dimers formations for the designed dyes with different anchoring groups both in the face-to-face and side-by-side ways. For this, we considered six dimer structures of designed dyes consisting of three different acceptor groups (CDM, TP and CDT) and two anchoring groups (COOH and CSSH). In face-to-face case, we considered two types such as Head-to-Head and Head-to-Tail type of dimers. The designed dimers both side-by-side and face-to-face are optimized using both B3LYP and ωB97XD functionals using 6-31G* basis set and optimized dimer structures for side-by-side and face-to-face are shown in Figures 5-7.

The intermolecular interaction energies (ΔE_{int}) were calculated as the energy difference between the isolated monomer and the dimer. We used the counterpoise (CP)[49, 50] method to eliminate the basis set superposition error (BSSE) in the calculation of interaction

energies. The calculated hydrogen bond distances and BSSE corrected interaction energies for both face-to-face and side-by-side dimers at ωB97XD/6-31G* are given in Tables 4 and 5, respectively. Previously, Malenov, et.al.,[51, 52] found that interaction energies for the stacked model systems calculated using the local correlated hybrid GGA with D2 dispersion correction ωB97XD method agree well with the CCSD(T)/CBS energies. From Tables 4 and 5, it can be seen that, the face-to-face dimers are more stable than the side-by-side dimers. Further, from Table 5, we observed a relatively weak interaction between the dimers containing CSSH anchoring groups, as supported by relatively low interaction energy than the COOH group and this is consistent with the intermolecular distances. The calculated average S···H bond distances (~2.57 Å) are longer than the O···H distances (1.67 Å), which leads to the smaller interaction energies for the dyes with CSSH anchoring group than the COOH group dimers. The accuracy of this method in predicting the hydrogen bond strengths are confirmed in recent study of Buytendyk.et.al.[53] Previously, Wenger et.al[54] reported that hydrogen bonding increases dye aggregation and recently, Dell'Orto and co-workers[55] confirmed in their study on N719 dye that the aggregation mainly arises through the intermolecular hydrogen bonding. It has been observed that the calculated S···H bond distances are slightly smaller than the net van der Walls radii of the binding atoms (2.70 Å),[56] indicating very weak intermolecular hydrogen bonding. Therefore, we expect that the

designed dyes with CSSH anchoring group may overturn the dye aggregation compared to the COOH group because of its weak intermolecular hydrogen bonding.

Further, in order to check the possibility of dimer formation for the designed dyes, we calculated the change in Gibbs free energy using $\Delta G = G_{AB} - (G_A + G_B)$, where G_{AB}, G_A and G_B are the Gibbs free energies of dimer and monomers A and B, respectively. We also included the BSSE correction for the calculation of ΔG and the calculated values of ΔG are given in Tables 4 and 5. It has been observed that the calculated ΔG values for all the designed dyes of face-to-face type dimers and the dyes containing COOH dimers in side-by side configuration are negative (ΔG<0), which indicate that the possibility of these interactions/reaction can occur at higher temperatures. Whereas, the change in Gibbs free energies for the dimers of dyes with CSSH anchoring group in side-by-side configuration are positive, which reveal that even at higher temperatures, the possibility of dimer formation for this dyes are comparatively less than others. The above results show that the dye aggregation due to the formation of dye dimers via intermolecular interaction is less in the dyes with CSSH anchoring group.

Furthermore, recent studies of Feng et.al,[20, 57] confirm that the structure of the dye in dimers also limits the absorption spectra and hence we also investigated the dimeric configurations by analyzing the dihedral angles between the different units in the dimer structures and that of monomers. The schematic representation of the selected dihedral angles

is shown in Figure 8 and the calculated dihedral angle values are given in Table S4 of supporting information. We noticed that the variation of these dihedral angels from monomer to dimer is very less in the case of dyes with CSSH anchoring group compared to COOH anchoring group, which indicate that the dyes of dimer with CSSH groups are having more planar structure than COOH, which leads to suppress the dye aggregation. The above results agree with the optimized dimeric structures of the designed dyes. As can be seen from the figure 6, the distance between two CSSH groups are relatively larger compared with the distance between the COOH groups, which can avoid the intermolecular interactions. We also calculated the hydrogen bond distances between the individual monomers in the Head to Head dimeric configuration of the designed dyes and the values are given in Table S5 of supporting information. We found that, either one of the considered hydrogen bond distance in the dyes with COOH anchoring group is in the range of ~2 Å, which indicate that there is a hydrogen bond formation between the monomer dyes. Whereas, all the hydrogen bond distances are comparatively longer (~3 - 6 Å) in the dimers having CSSH anchoring group, which supports the earlier results that possibility of dye aggregation in CSSH anchoring group dyes is less than the others.

To gain insights about the possible aggregation of the designed dyes due to intermolecular hydrogen bonding (O···H and S···H), the radial distribution functions (RDFs) between the dye monomers are calculated from the MD simulations. The RDF can provide an

approximate estimation of interaction of dye molecules at a particular distance. The calculated RDF for the interactions between O & H atoms and S & H atoms are shown in Figure 9. Fig 9a illustrates that the first peak of RDF for O···H and S···H interactions at an average time of 500 ps located at around 1.75 and 2.25 Å, respectively, which indicates that S···H interaction is significantly weaker than the O···H interactions. From Fig 9b, it has been observed that, the position of the peak and its trend does not change with time evolution, but the amplitude decreased significantly. Whereas in Fig 9a, even at 2000 ps time, there is large amplitude peak located around 4 Å. These results clearly indicate that, even after 2000 ps the dyes with COOH anchoring groups are interacted with each other, which can increase dye aggregation. On the other hand, after certain period of time, the dyes with CSSH anchoring groups tend to keep away from each other and hence the intermolecular distance increases between those dyes. Therefore, we may expect that the designed dyes containing CSSH anchoring group can bind strongly with the semiconductor surface than the other dyes and it can inject excited electrons efficiently due to the less aggregation effect. From the above results we found that the dye aggregation can be suppressed not only by means of adding additives but also by changing the appropriate anchoring groups while designing the efficient sensitizers for the DSSC applications.

4. Conclusions:

In summary, we have designed organic dyes with different acceptor and anchoring groups and studied their optoelectronic properties using DFT and TDDFT methods. Our calculated results indicate that the dyes with CSSH anchoring groups are having improved spectral properties such as considerable redshift with an increase in intensity in the absorption spectra compared to the dyes with other anchoring groups. We also confirm that the inclusion of cyano group into the anchoring part enhances the absorption spectra of the designed sensitizers. It has also been demonstrated that the formation of dye dimers through intermolecular hydrogen bonding interactions by MD simulations. We found that the intermolecular hydrogen bonds in the dyes with CSSH anchoring groups are much weaker than the COOH dyes, which indicate that aggregation due to intermolecular hydrogen bonding were minimized in those dyes. We found that the dye aggregation can be suppressed not only by means of adding additives but also by changing the anchoring part of the dyes. This theoretical work could give an idea to suppress the dye aggregation while designing the efficient sensitizers for the practical application of DSSCs.

Acknowledgements: We gratefully acknowledge Ministry of Science and Technology for financial support (MOST 104-2113-M-011-002 and MOST 103-2219-M-011-002). We are also thankful to the National Center of High-Performance Computing (NCHC) for donating computer time and facilities.

Supporting Materials: Supporting results (Tables S1-S4 and Figures S1-S3) are shown.

References:

1. B. O'regan and M. Grfitzeli, *Nature*, 1991, 353, 737.
2. M. Gratzel, *Nature*, 2001, 414, 338.
3. S. Mathew, A. Yella, P. Gao, R. Humphry-Baker, B. F. E. Curchod, N. Ashari-Astani, I. Tavernelli, U. Rothlisberger, M. K. Nazeeruddin and M. Gratzel, *Nature Chemistry*, 2014, 6, 242.
4. N. Santhanamoorthi, L. Kuan-Hwa, F. Taufany and J.-C. Jiang, *Phys. Chem. Chem. Phys.*, 2014, 16, 15389.
5. C.-Y. Tseng, F. Taufany, S. Nachimuthu, J.-C. Jiang and D.-J. Liaw, *Org. Electron.*, 2014, 15, 1205.
6. H. Imahori, Y. Matsubara, H. Iijima, T. Umeyama, Y. Matano, S. Ito, M. Niemi, N. V. Tkachenko and H. Lemmetyinen, *J. Phys. Chem. C*, 2010, 114, 10656.
7. A. Mishra, M. K. Fischer and P. Bäuerle, *Angew. Chem. Int. Ed.*, 2009, 48, 2474.
8. Y. Sakuragi, X. F. Wang, H. Miura, M. Matsui and T. Yoshida, *J. Photoch. Photobio. A*, 2010, 216, 1.
9. H. J. Snaith, C. S. Karthikeyan, A. Petrozza, J. Teuscher, J. E. Moser, M. K. Nazeeruddin, M. Thelakkat and M. Gratzel, *J. Phys. Chem. C*, 2008, 112, 7562.
10. H. N. Tian, X. C. Yang, R. K. Chen, R. Zhang, A. Hagfeldt and L. C. Sunt, *J. Phys. Chem. C*, 2008, 112, 11023.
11. S. Tatay, S. A. Haque, B. O'Regan, J. R. Durrant, W. J. H. Verhees, J. M. Kroon, A. Vidal-Ferran, P. Gavina and E. Palomares, *J. Mater. Chem.*, 2007, 17, 3037.
12. A. Ehret, L. Stuhl and M. T. Spitler, *J. Phys. Chem. B*, 2001, 105, 9960.
13. D. Heredia, J. Natera, M. Gervaldo, L. Otero, F. Fungo, C. Y. Lin and K. T. Wong, *Org. Lett.*, 2010, 12, 12.
14. Z. J. Ning, Q. Zhang, W. J. Wu, H. C. Pei, B. Liu and H. Tian, *J. Org. Chem.*, 2008, 73, 3791.
15. N. Cho, H. Choi, D. Kim, K. Song, M. S. Kang, S. O. Kang and J. Ko, *Tetrahedron*, 2009, 65, 6236.
16. S. Ito, H. Miura, S. Uchida, M. Takata, K. Sumioka, P. Liska, P. Comte, P. Pechy and M. Graetzel, *Chem. Commun.*, 2008, DOI: Doi 10.1039/B809093a, 5194.
17. N. R. Neale, N. Kopidakis, J. van de Lagemaat, M. Gratzel and A. J. Frank, *J. Phys. Chem. B*, 2005, 109, 23183.
18. S. Sakaguchi, S. S. Pandey, K. Okada, Y. Yamaguchi and S. Hayase, *Appl. Phys. Express*, 2008, 1.
19. N. Santhanamoorthi, K.-H. Lai, F. Taufany and J.-C. Jiang, *J. Power Sources*, 2013, 242, 464.
20. S. Feng, Q. S. Li, L. N. Yang, Z. Z. Sun, T. A. Niehaus and Z. S. Li, *J. Power Sources*,

2015, 273, 282.
21. H. Kusama and K. Sayama, *J. Phys. Chem. C*, 2012, 116, 23906.
22. A. D. Becke, *J. Chem. Phys.*, 1993, 98, 5648.
23. J. D. Chai and M. Head-Gordon, *J. Chem. Phys.*, 2008, 128.
24. J. D. Chai and M. Head-Gordon, *Phys. Chem. Chem. Phys.*, 2008, 10, 6615.
25. Y. Zhao and D. G. Truhlar, *Theor. Chem. Acc.*, 2008, 120, 215.
26. T. Yanai, D. P. Tew and N. C. Handy, *Chem. Phys. Lett.*, 2004, 393, 51.
27. V. A. Rassolov, M. A. Ratner, J. A. Pople, P. C. Redfern and L. A. Curtiss, *J. Comput. Chem.*, 2001, 22, 976.
28. A. D. Becke, *J. Chem. Phys.*, 1993, 98, 1372.
29. D. P. Hagberg, T. Marinado, K. M. Karlsson, K. Nonomura, P. Qin, G. Boschloo, T. Brinck, A. Hagfeldt and L. Sun, *The Journal of organic chemistry*, 2007, 72, 9550.
30. V. Barone and M. Cossi, *J. Phys. Chem. A*, 1998, 102, 1995.
31. M. Cossi, N. Rega, G. Scalmani and V. Barone, *J. Comput. Chem.*, 2003, 24, 669.
32. F. Turecek, *J. Phys. Chem. A*, 2015, 119, 10101.
33. H. Li, R. Nieman, A. J. A. Aquino, H. Lischka and S. Tretiak, *J. Chem. Theory Comput.*, 2014, 10, 3280.
34. S. I. Gorelsky and A. B. P. Lever, *J. Organomet. Chem.*, 2001, 635, 187.
35. S. I. Gorelsky, SWizard program,
36. M. J. Frisch, G. W. Trucks, H. B. Schlegel, G. E. Scuseria, M. A. Robb, J. R. Cheeseman, G. Scalmani, V. Barone, B. Mennucci, G. A. Petersson, H. Nakatsuji, M. Caricato, X. Li, H. P. Hratchian, A. F. Izmaylov, J. Bloino, G. Zheng, J. L. Sonnenberg, M. Hada, M. Ehara, K. Toyota, R. Fukuda, J. Hasegawa, M. Ishida, T. Nakajima, Y. Honda, O. Kitao, H. Nakai, T. Vreven, J. A. Montgomery, Jr.; , J. E. Peralta, F. Ogliaro, M. Bearpark, J. J. Heyd, E. Brothers, K. N. Kudin, V. N. Staroverov, R. Kobayashi, J. Normand, K. Raghavachari, A. Rendell, J. C. Burant, S. S. Iyengar, J. Tomasi, M. Cossi, N. Rega, N. J. Millam, M. Klene, J. E. Knox, J. B. Cross, V. Bakken, C. Adamo, J. Jaramillo, R. Gomperts, R. E. Stratmann, O. Yazyev, A. J. Austin, R. Cammi, C. Pomelli, J. W. Ochterski, R. L. Martin, K. Morokuma, V. G. Zakrzewski, G. A. Voth, P. Salvador, J. J. Dannenberg, S. Dapprich, A. D. Daniels, O. Farkas, J. B. Foresman, J. V. Ortiz, J. Cioslowski and D. J. Fox, Gaussian 09, revision A.1; ,
37. Accelrys Software Inc., Materials Studio Release Notes,
38. S. W. Bunte and H. Sun, *J. Phys. Chem. B*, 2000, 104, 2477.
39. H. Sun, P. Ren and J. R. Fried, *Comput. Theor. Polym. Sci.*, 1998, 8, 229.
40. H. Sun, *Macromolecules*, 1995, 28, 701.
41. N. Santhanamoorthi, C. M. Lo and J. C. Jiang, *J. Phys. Chem. Lett.*, 2013, 4, 524.
42. W. M. Campbell, K. W. Jolley, P. Wagner, K. Wagner, P. J. Walsh, K. C. Gordon, L.

Schmidt-Mende, M. K. Nazeeruddin, Q. Wang, M. Gratzel and D. L. Officer, *J. Phys. Chem. C*, 2007, 111, 11760.

43. R. M. Ma, P. Guo, H. J. Cui, X. X. Zhang, M. K. Nazeeruddin and M. Gratzel, *J. Phys. Chem. A*, 2009, 113, 10119.
44. M. Pastore and F. De Angelis, *ACS Nano*, 2010, 4, 556.
45. F. Wurthner, T. E. Kaiser and C. R. Saha-Moller, *Angew. Chem. Int. Ed.*, 2011, 50, 3376.
46. V. Karunakaran, D. D. Prabhu and S. Das, *J. Phys. Chem. C*, 2013, 117, 9404.
47. E. E. Jelley, *Nature* 1936, 138, 1009.
48. E. E. Jelley, *Nature*, 1937, 139, 631.
49. S. Simon, M. Duran and J. J. Dannenberg, *J. Chem. Phys.*, 1996, 105, 11024.
50. S. F. Boys and F. Bernardi, *Mol. Phys.*, 2002, 100, 65.
51. D. P. Malenov, D. B. Ninkovic and S. D. Zaric, *ChemPhysChem*, 2015, 16, 761.
52. D. P. Malenov, D. B. Ninkovic, D. N. Sredojevic and S. D. Zaric, *ChemPhysChem*, 2014, 15, 2458.
53. A. M. Buytendyk, J. D. Graham, K. D. Collins, K. H. Bowen, C. H. Wu and J. I. Wu, *Phys. Chem. Chem. Phys.*, 2015, 17, 25109.
54. B. Wenger, M. Gratzel and J. E. Moser, *J. Am. Chem. Soc.*, 2005, 127, 12150.
55. E. Dell'Orto, L. Raimondo, A. Sassella and A. Abbotto, *J. Mater. Chem.*, 2012, 22, 11364.
56. A. Bondi, *J. Phys. Chem.*, 1964, 68, 441.
57. S. Feng, Q. S. Li, P. P. Sun, T. A. Niehaus and Z. S. Li, *Acs Appl Mater Inter*, 2015, 7, 22504.

Figure Captions:

Fig. 1. Sketch of molecular structures for donor (MPBA), π-linker (T), and different acceptors (CDM, TP and CDT) and anchoring groups (COOH, CSSH, PO_3H_2 and SO_3H) considered in this work.

Fig. 2. The simulated UV/vis absorption spectra for the designed dyes with (a) COOH (b) PO_3H_2 (c) SO_3H and (d) CSSH anchoring groups at ωB97XD/6-31G* level of theory. (The dyes without CN groups are shown in solid lines, and with CN groups are shown in dashed lines)

Fig. 3. Isodensity plots of selected frontier molecular orbitals of the designed dyes with different acceptors and anchoring (COOH and CSSH) groups. The calculations were performed by ωB97XD/6-31G* level of theory and the isovalue is 0.02 a.u.

Fig. 4. Molecular orbital energy levels of designed dyes with different acceptors and anchoring groups (COOH and CSSH) calculated at ωB97XD/6-31G* level of theory.

Fig. 5. Optimized dimer geometries of the designed dyes in side-by-side configuration. (Atoms with white, gray, blue, red, and yellow represent H, C, N, O, and S, respectively. Intermolecular hydrogen bonds are shown in dashed lines.)

Fig. 6. Optimized dimer geometries of the designed dyes in face-to-face (Head to Head) configuration. (Atoms with white, gray, blue, red, and yellow represent H, C, N, O, and S, respectively.)

Fig. 7. Optimized dimer geometries of the designed dyes in face-to-face (Head to Tail) configuration. (Atoms with white, gray, blue, red, and yellow represent H, C, N, O, and S, respectively.)

Fig.8. The schematic representation of the selected dihedral angles (θ_1-θ_3) between the different units of the designed dyes. (D, π, Acc. and An refer to Donor, π-bridge, Acceptor, and Anchoring groups, respectively)

Fig. 9. The calculated radial distribution function for the intermolecular O···H and S···H bonds of the designed dyes with TP acceptor and (a) COOH and (b) CSSH anchoring groups.

Table 1. The calculated absorption energies (λ in nm), oscillator strength (*f* in a.u.) and the corresponding MO transitions of designed dyes with COOH anchoring group at ωB97XD/6-31G* level of theory.

Dyes	State	λ	*f*	Transition assignment
Dπ-CDM	S0→S1	648.3	0.13	H-1->L+0 (67%)
	S0→S3	346.4	1.63	H-1->L+1 (27%), H-0->L+1 (22%), H-0->L+2 (21%)
Dπ-^{CN}CDM	S0→S1	635.7	0.19	H-1->L+0 (64%), H-0->L+0 (19%)
	S0→S3	364.2	1.40	H-1->L+1 (37%), H-0->L+1 (19%)
Dπ-TP	S0→S1	495.7	0.86	H-0->L+0 (51%), H-1->L+0 (44%)
	S0→S4	304.7	0.57	H-1->L+1 (31%), H-0->L+1 (31%)
Dπ-^{CN}TP	S0→S1	520.0	1.02	H-0->L+0 (52%), H-1->L+0 (43%)
	S0→S4	319.4	0.46	H-1->L+1 (48%), H-0->L+1 (31%)
Dπ-CDT	S0→S1	392.8	2.03	H-1->L+0 (44%), H-0->L+0 (39%)
Dπ-^{CN}CDT	S0→S1	420.2	1.98	H-1->L+0 (53%), H-0->L+0 (30%)

*H and L represent HOMO and LUMO, respectively.

Table 2. The calculated absorption energies (λ in nm), oscillator strength (*f* in a.u.) and the corresponding MO transitions of designed dyes with CSSH anchoring group at ωB97XD/6-31G* level of theory.

Dyes	State	λ	*f*	Transition assignment
Dπ-CDM	S0→S1	656.0	0.18	H-1->L+0 (66%)
	S0→S4	374.1	1.13	H-1->L+1 (36%)
Dπ-^{CN}CDM	S0→S1	641.6	0.27	H-1->L+0 (62%), H-0->L+0 (19%)
	S0→S3	409.5	1.30	H-0->L+0 (34%), H-1->L+1 (28%)
Dπ-TP	S0→S1	531.7	1.14	H-0->L+0 (52%), H-1->L+0 (41%)
	S0→S5	343.0	0.38	H-1->L+1 (42%), H-0->L+1 (34%)
Dπ-^{CN}TP	S0→S1	553.8	1.30	H-0->L+0 (54%), H-1->L+0 (40%)
	S0→S5	349.7	0.37	H-1->L+1 (50%), H-0->L+1 (34%)
Dπ-CDT	S0→S2	436.1	2.09	H-1->L+0 (49%), H-0->L+0 (32%)
	S0→S3	332.4	0.26	H-0->L+1 (43%)
Dπ-^{CN}CDT	S0→S2	459.0	2.13	H-1->L+0 (56%), H-0->L+0 (26%)
	S0→S3	342.6	0.20	H-0->L+1 (32%)

*H and L represent HOMO and LUMO, respectively.

Table 3. Molecular Orbital Composition (in %) of the two highest occupied and two lowest unoccupied molecular orbitals of designed dyes with COOH and CSSH anchoring groups calculated at ωB97XD/6-31G* level of theory.

Dyes	Orbital	COOH series				CSSH series			
		D	π	Acc.	Anc.	D	π	Acc.	Anc.
Dπ-CDM	L+1	2	8	78	12	0	1	56	43
	L+0	0	1	98	1	0	2	94	4
	H-0	84	11	5	0	84	11	5	0
	H-1	22	23	54	1	21	21	54	4
Dπ-^{CN}CDM	L+1	1	2	88	9	0	1	68	31
	L+0	0	2	97	1	0	2	92	6
	H-0	86	9	5	0	86	9	5	0
	H-1	24	25	50	1	23	24	50	3
Dπ-TP	L+1	5	7	78	10	1	2	60	37
	L+0	3	13	80	4	2	12	67	19
	H-0	73	14	12	1	71	15	12	2
	H-1	33	21	44	2	33	17	42	8
Dπ-^{CN}TP	L+1	0	0	92	8	0	1	67	32
	L+0	3	14	79	4	3	13	69	15
	H-0	76	14	10	0	74	13	11	2
	H-1	31	22	45	2	30	19	43	8
Dπ-CDT	L+1	23	35	35	7	11	30	43	16
	L+0	3	10	78	9	1	3	57	39
	H-0	71	15	14	0	69	14	16	1
	H-1	28	10	60	2	30	9	56	5
Dπ-^{CN}CDT	L+1	19	36	41	4	11	27	42	20
	L+0	1	6	85	8	1	2	66	31
	H-0	77	13	10	0	78	12	10	0
	H-1	24	15	60	1	23	13	59	5

H and L refer to the HOMO and LUMO, respectively

D, π, Acc. and Anc. denote donor, π-bridge, acceptor group and anchoring groups, respectively

Table 4. Calculated interaction energies (ΔE_{int} in eV), and change in Gibbs free energies (ΔG in eV) for the designed dye dimers in face-to-face configuration.

Parameters	Type*	COOH Series			CSSH Series		
		Dπ-CDM	**Dπ-TP**	**Dπ-CDT**	**Dπ-CDM**	**Dπ-TP**	**Dπ-CDT**
ΔE_{int}	H - H	-1.30	-1.02	-1.15	-1.32	-1.13	-1.19
	H - T	-1.36	-0.86	-1.04	-1.30	-1.00	-1.04
ΔG	H - H	-0.34	-0.02	-0.15	-0.30	-0.17	-0.22
	H - T	-0.46	-0.04	-0.11	-0.32	-0.10	-0.17

*H-H : Head-to-Head, H-T : Head-to-Tail

Table 5. Calculated intermolecular distance (D in Å), interaction energies (ΔE_{int} in eV) and change in Gibbs free energies (ΔG in eV) for the designed dye dimers in side-by-side configuration.

Parameters	COOH Series			CSSH Series		
	Dπ-CDM	**Dπ-TP**	**Dπ-CDT**	**Dπ-CDM**	**Dπ-TP**	**Dπ-CDT**
D	1.669	1.670	1.668	2.560	2.574	2.551
ΔE_{int}	-0.73	-0.71	-0.74	-0.21	-0.22	-0.22
ΔG	-0.19	-0.11	-0.11	0.26	0.32	0.30

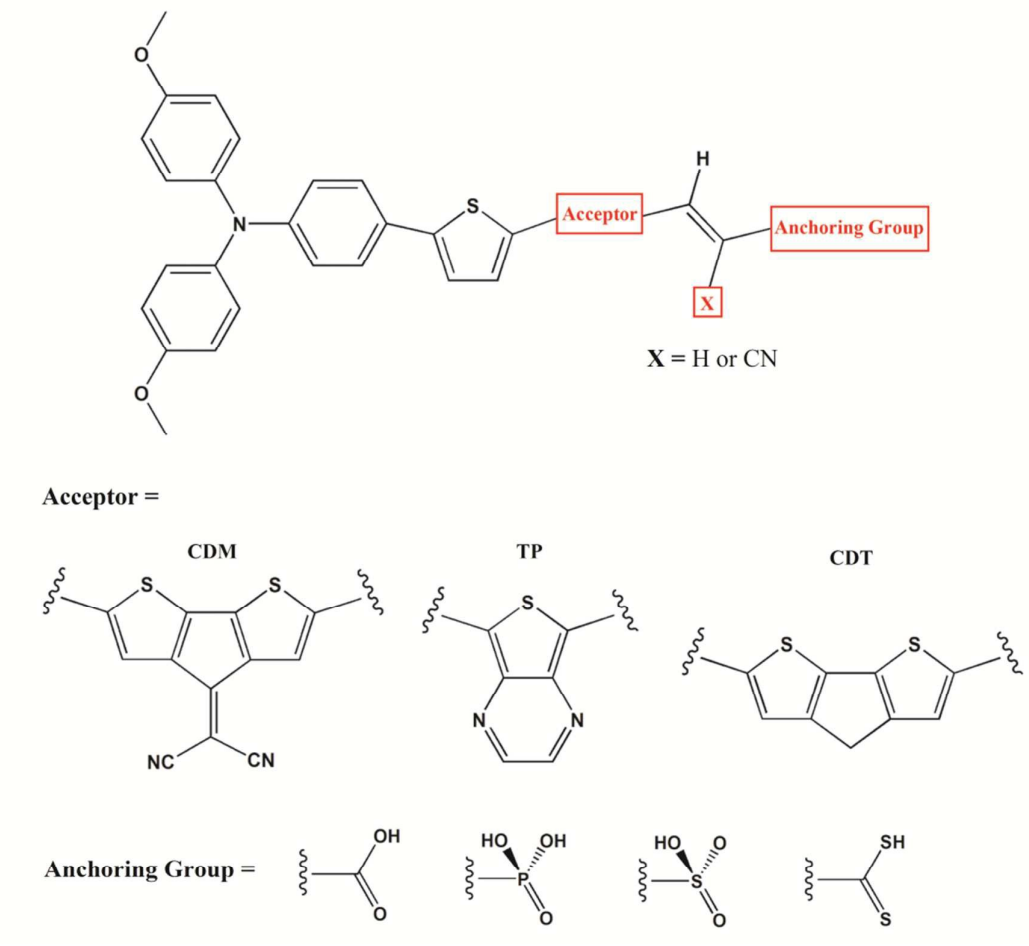

Fig 1.

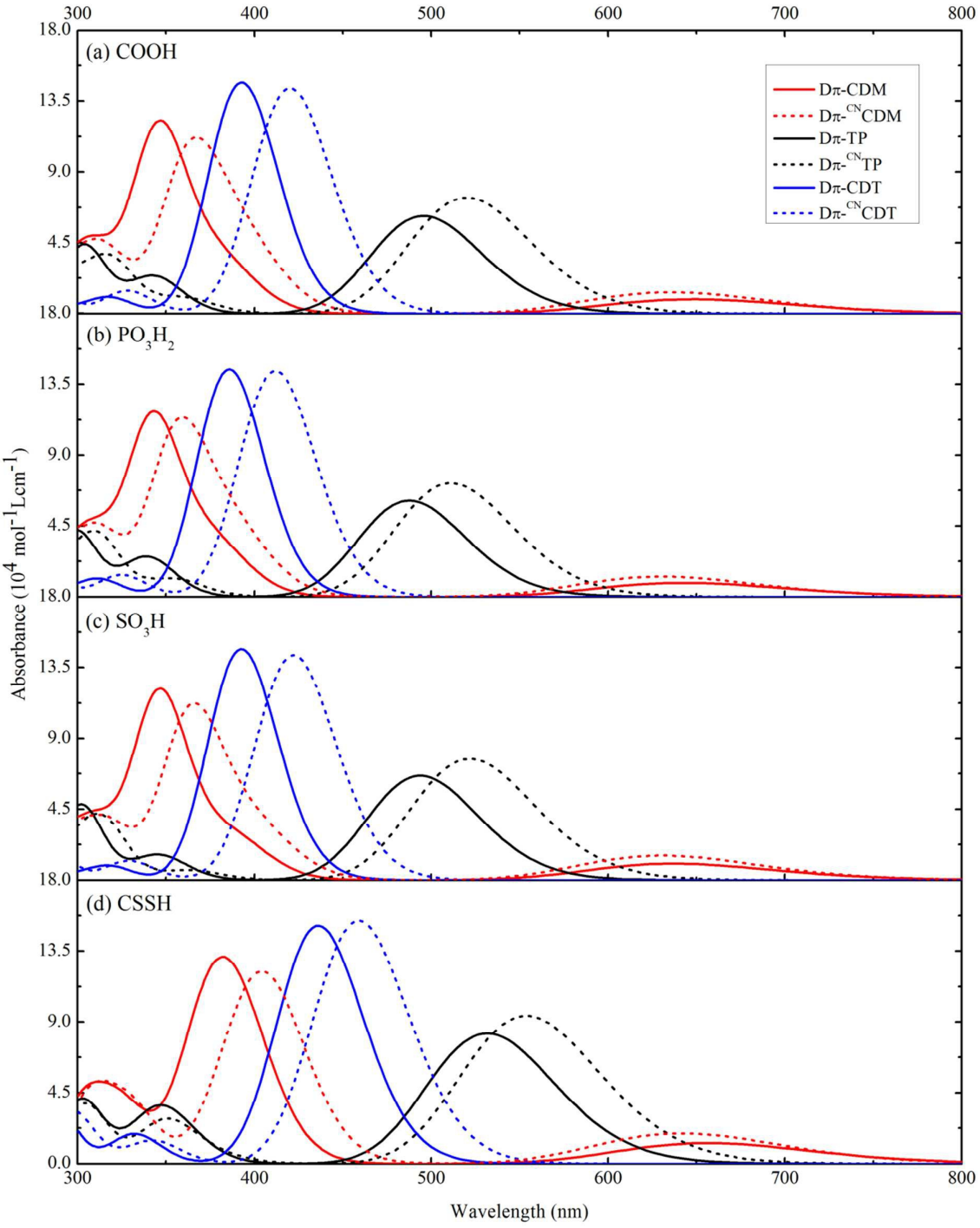

Fig. 2.

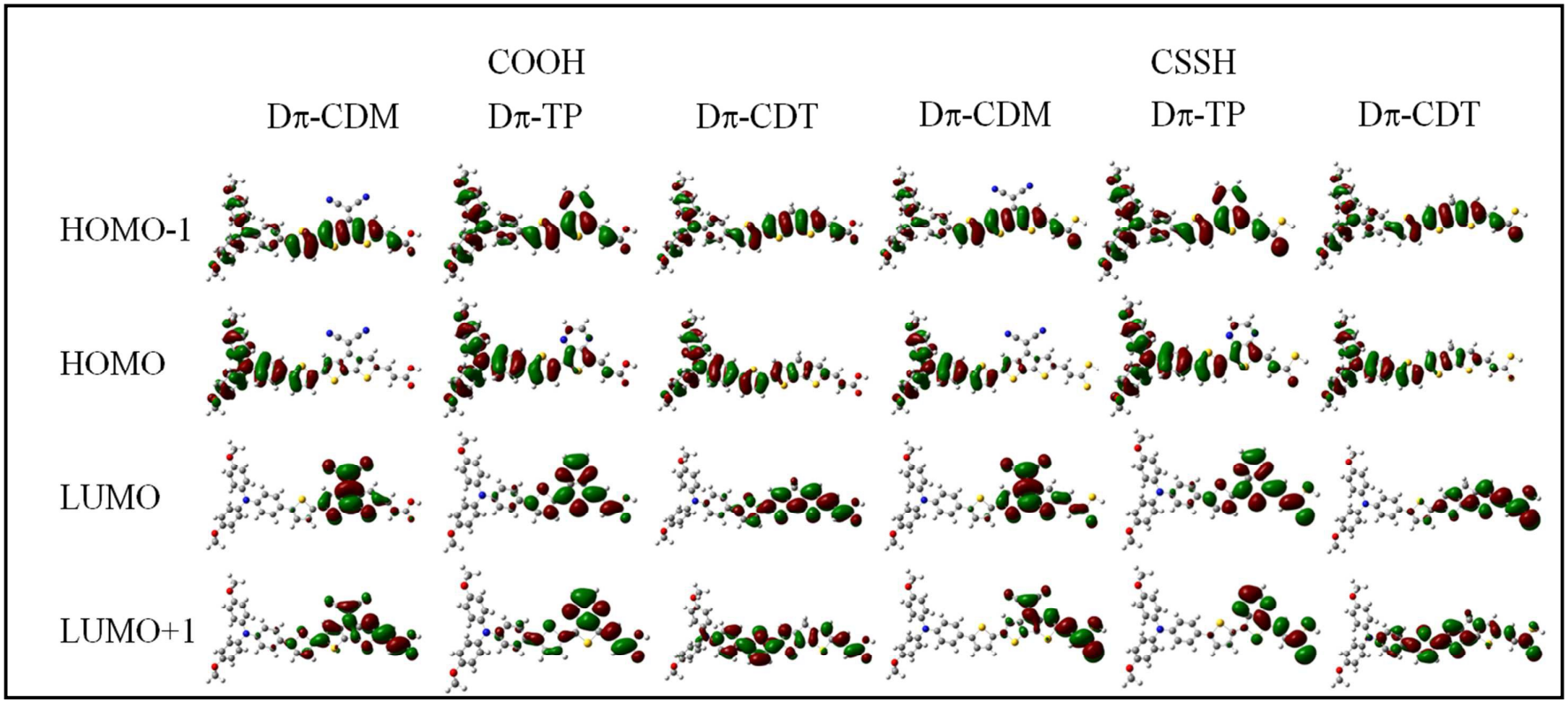

Fig. 3.

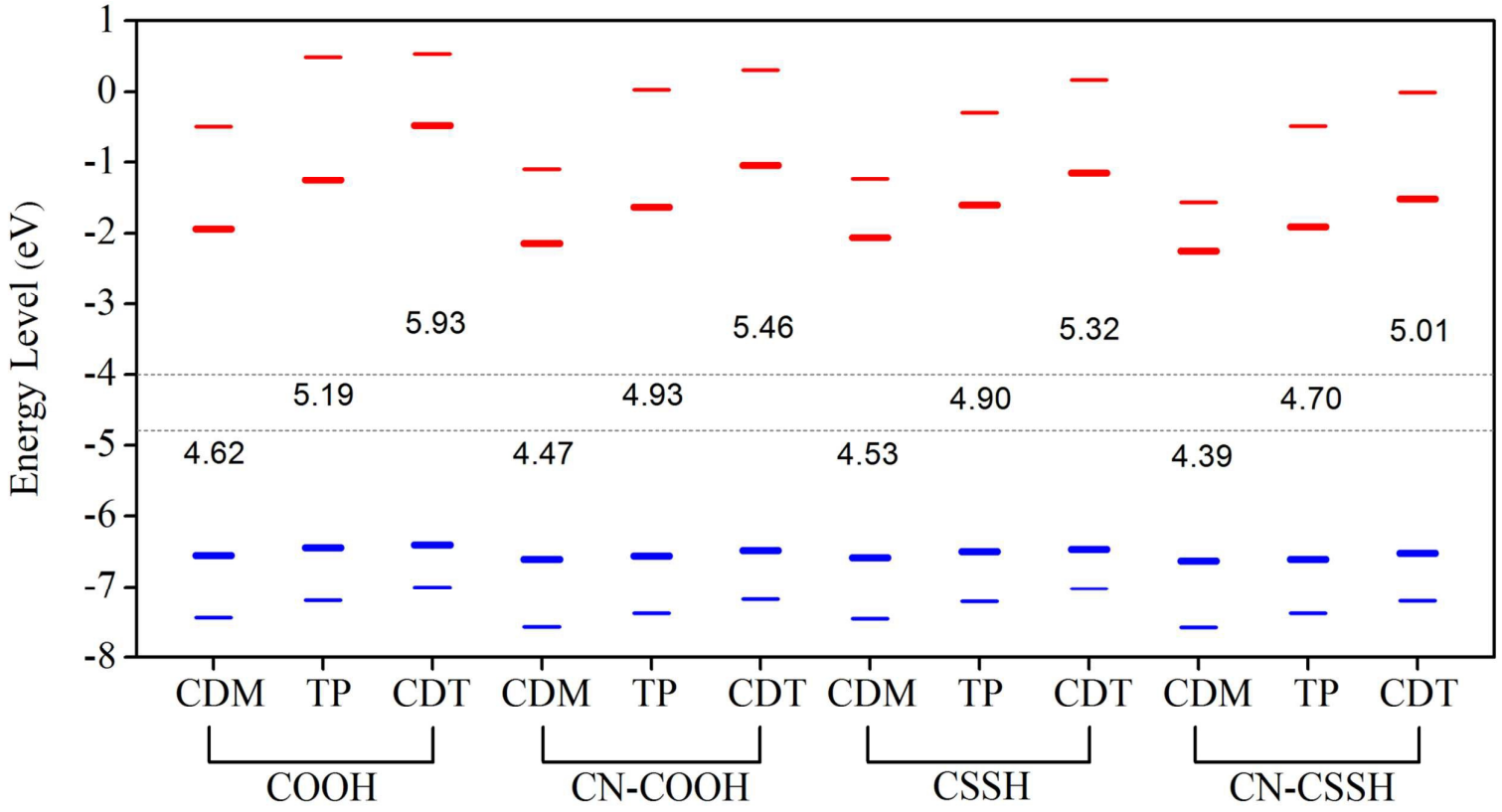

Fig. 4.

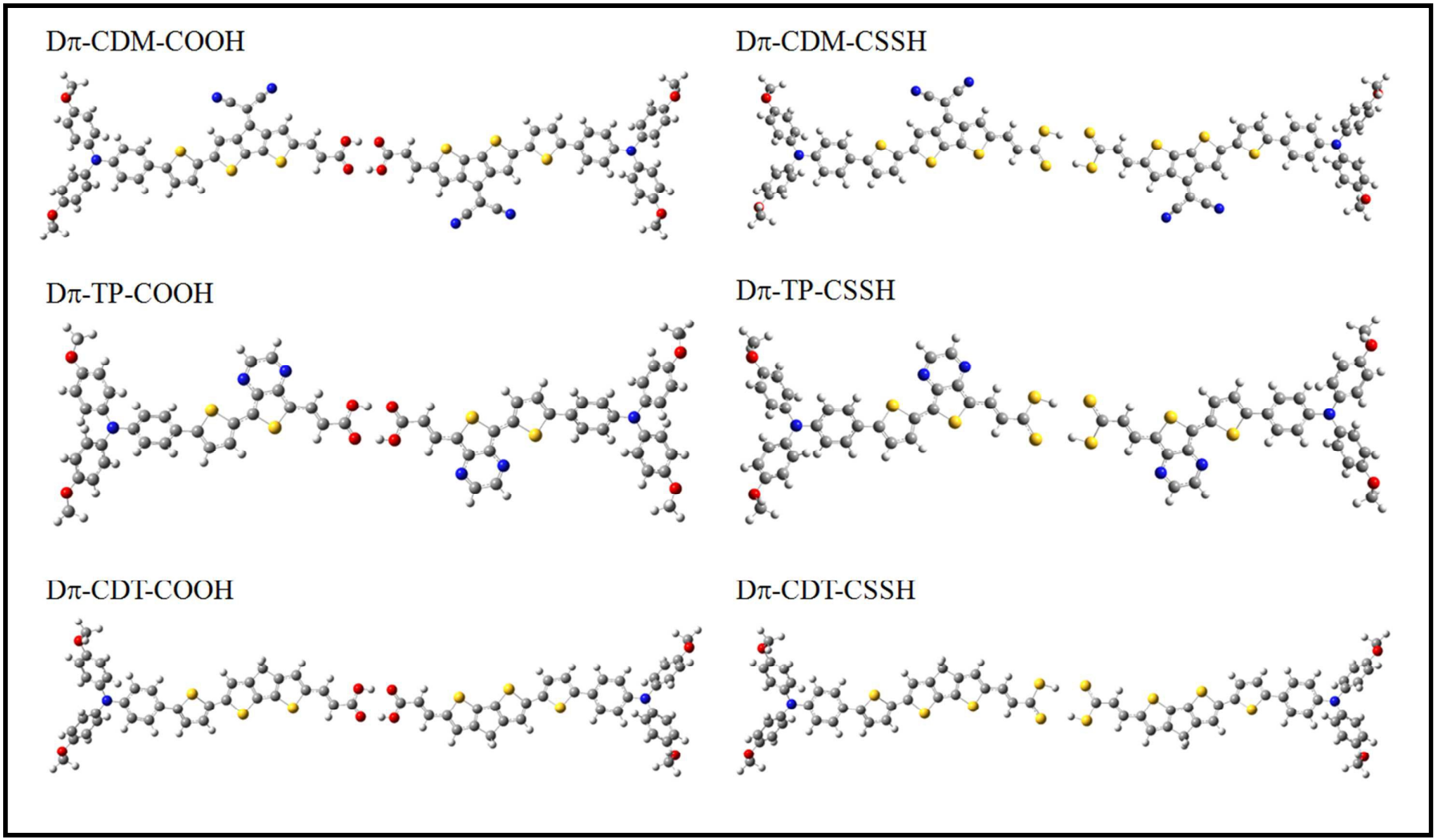

Fig. 5.

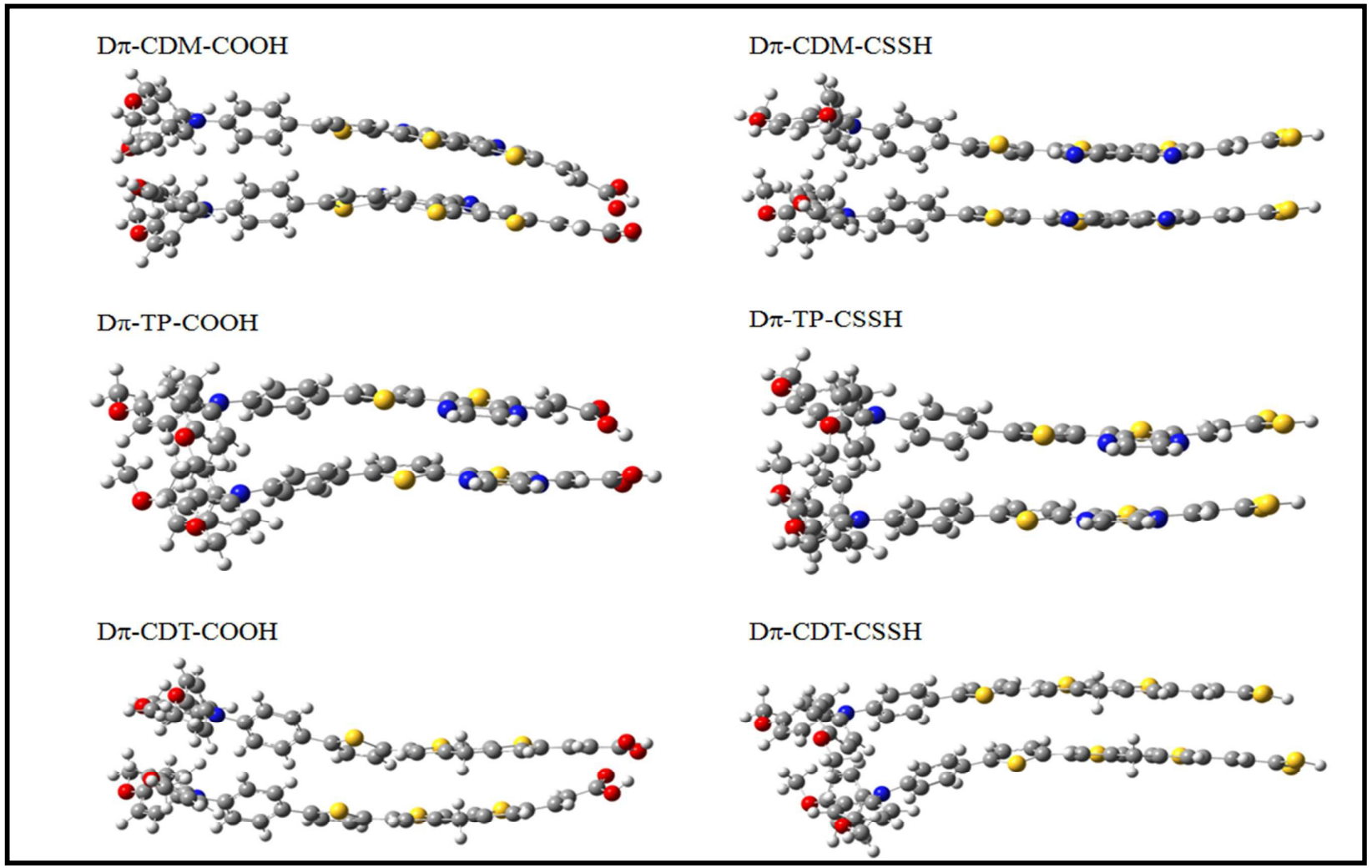

Fig. 6

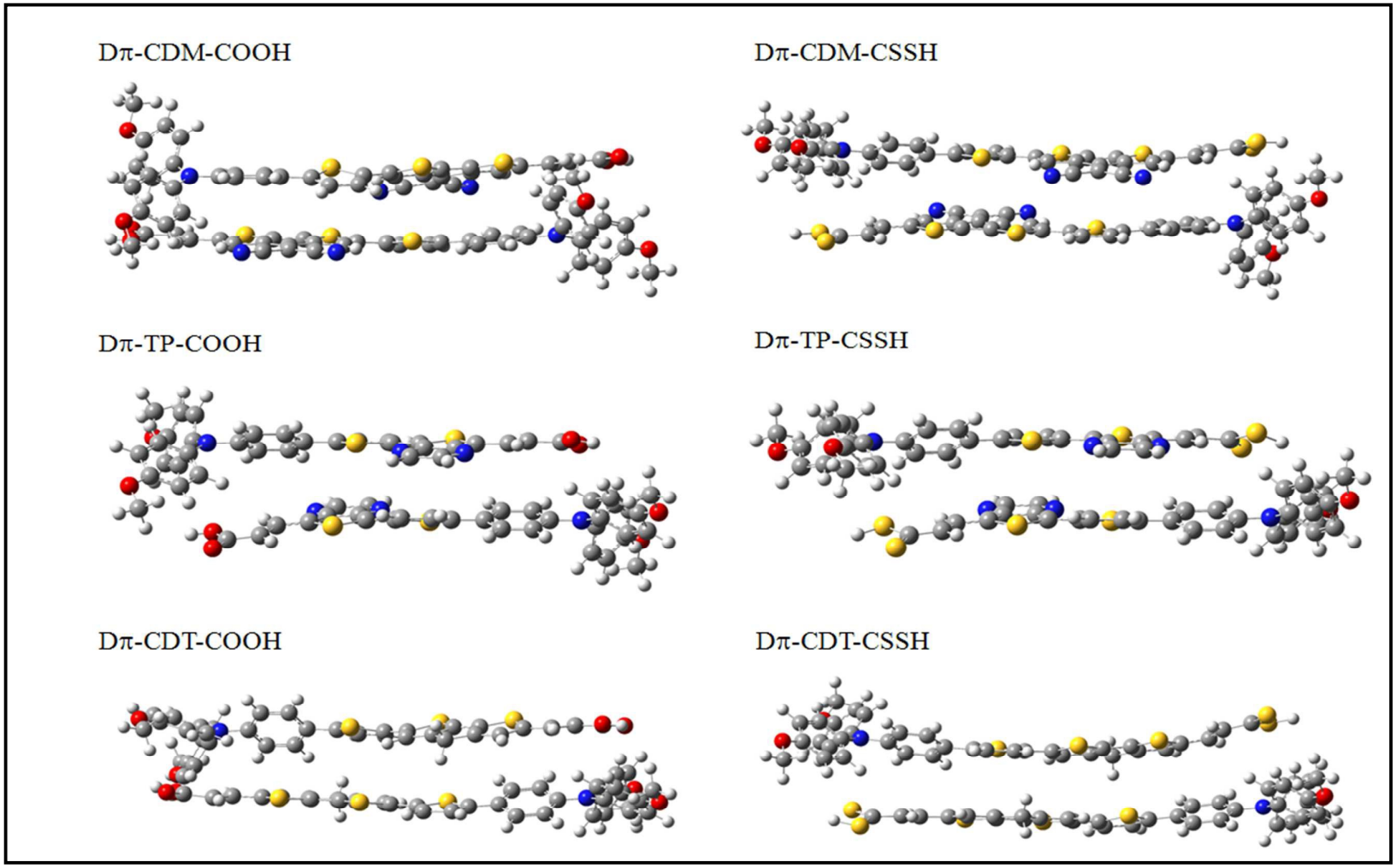

Fig. 7

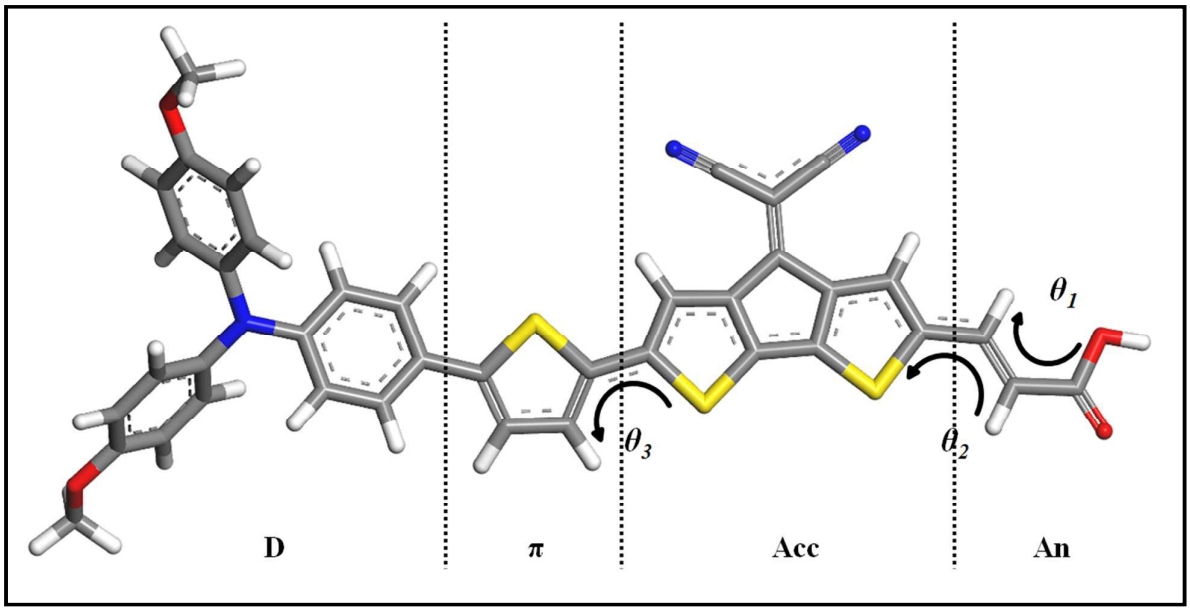

Fig. 8

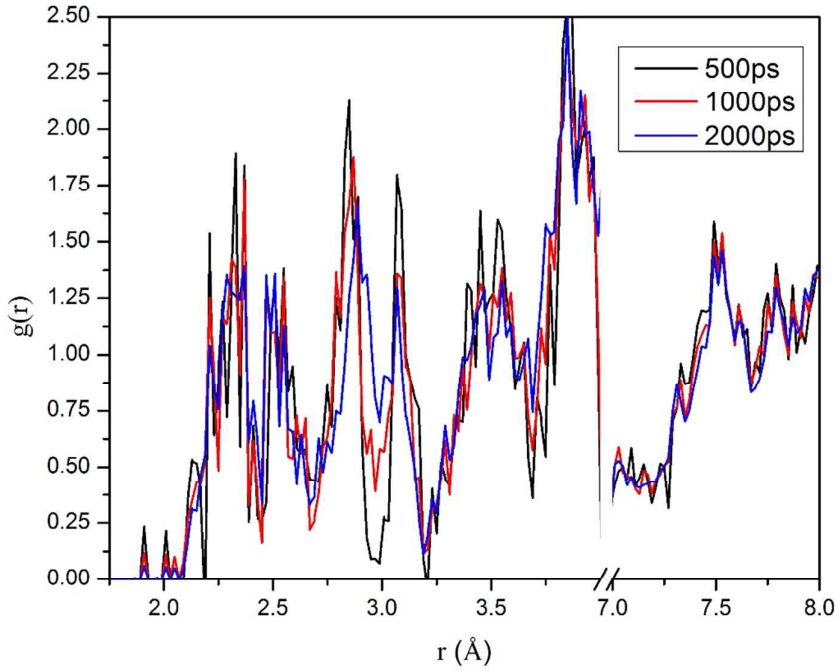

(a)

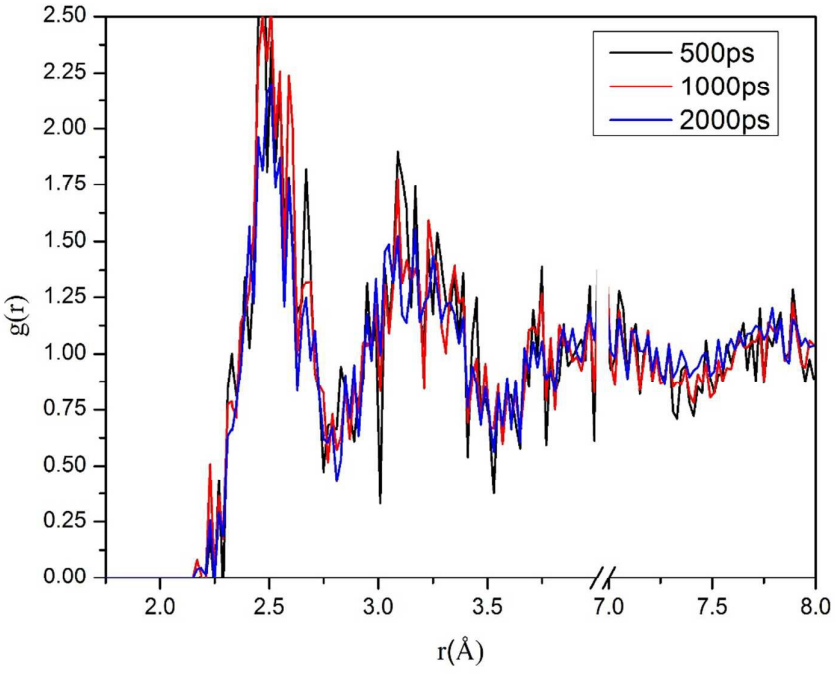

(b)

Fig. 9.

Graphical Abstract:

Efficient organic sensitizers with improved spectral properties and less aggregation have been proposed for practical DSSC based on theoretical calculations.